The Astrophysical Journal Letters, 734:L27 (6pp), 2011 June 20 doi:10.1088/2041-8205/734/2/L27

DETECTION OF HIGH-ENERGY GAMMA-RAY EMISSION DURING THE X-RAY FLARING ACTIVITY IN GRB 100728A

A. A. Abdo[1,55], M. Ackermann[2], M. Ajello[2], L. Baldini[3], J. Ballet[4], G. Barbiellini[5,6], M. G. Baring[7], D. Bastieri[8,9], K. Bechtol[2], R. Bellazzini[3], B. Berenji[2], P. N. Bhat[10], E. Bissaldi[11], R. D. Blandford[2], E. Bonamente[12,13], J. Bonnell[14,15], A. W. Borgland[2], A. Bouvier[16], J. Bregeon[3], M. Brigida[17,18], P. Bruel[19], R. Buehler[2], S. Buson[8,9], G. A. Caliandro[20], R. A. Cameron[2], P. A. Caraveo[21], J. M. Casandjian[4], C. Cecchi[12,13], E. Charles[2], A. Chekhtman[22,55], J. Chiang[2], S. Ciprini[13], R. Claus[2], V. Connaughton[10], J. Conrad[23,24,56], S. Cutini[25], A. de Angelis[26], F. de Palma[17,18], C. D. Dermer[27], E. do Couto e Silva[2], P. S. Drell[2], R. Dubois[2], C. Favuzzi[17,18], Y. Fukazawa[28], P. Fusco[17,18], F. Gargano[18], N. Gehrels[14], S. Germani[12,13], N. Giglietto[17,18], P. Giommi[25], F. Giordano[17,18], M. Giroletti[29], T. Glanzman[2], G. Godfrey[2], J. Granot[30], I. A. Grenier[4], S. Guiriec[10], D. Hadasch[20], Y. Hanabata[28], R. E. Hughes[31], G. Jóhannesson[32], A. S. Johnson[2], T. Kamae[2], H. Katagiri[28], J. Kataoka[33], M. Kerr[2], J. Knödlseder[34,35], M. Kuss[3], J. Lande[2], L. Latronico[3], S.-H. Lee[2], F. Longo[5,6], F. Loparco[17,18], B. Lott[36], P. Lubrano[12,13], M. N. Mazziotta[18], J. E. McEnery[14,15], P. Mészáros[37], P. F. Michelson[2], T. Mizuno[28], A. A. Moiseev[15,38], M. E. Monzani[2], A. Morselli[39], I. V. Moskalenko[2], S. Murgia[2], T. Nakamori[33], M. Naumann-Godo[4], P. L. Nolan[2], J. P. Norris[40], E. Nuss[41], T. Ohsugi[42], A. Okumura[43], N. Omodei[2], E. Orlando[2,44], W. S. Paciesas[10], V. Pelassa[41], M. Pesce-Rollins[3], M. Pierbattista[4], F. Piron[41], T. A. Porter[2], J. L. Racusin[14], S. Rainò[17,18], M. Razzano[3], S. Razzaque[1,55], A. Reimer[2,11], O. Reimer[2,11], L. C. Reyes[45], M. Roth[46], H. F.-W. Sadrozinski[16], C. Sgrò[3], E. J. Siskind[47], P. D. Smith[31], E. Sonbas[14,48,49], G. Spandre[3], P. Spinelli[17,18], M. Stamatikos[14,31], M. S. Strickman[27], H. Takahashi[42], T. Tanaka[2], Y. Tanaka[43], J. G. Thayer[2], J. B. Thayer[2], D. F. Torres[20,50], G. Tosti[12,13], E. Troja[14,57], T. Uehara[28], T. L. Usher[2], J. Vandenbroucke[2], V. Vasileiou[41], G. Vianello[2,51], N. Vilchez[34,35], V. Vitale[39,52], A. von Kienlin[44], A. P. Waite[2], P. Wang[2], B. L. Winer[31], K. S. Wood[27], R. Yamazaki[53], Z. Yang[23,24], M. Ziegler[16], and L. Piro[54]

[1] Center for Earth Observing and Space Research, College of Science, George Mason University, Fairfax, VA 22030, USA
[2] W. W. Hansen Experimental Physics Laboratory, Kavli Institute for Particle Astrophysics and Cosmology, Department of Physics and SLAC National Accelerator Laboratory, Stanford University, Stanford, CA 94305, USA
[3] Istituto Nazionale di Fisica Nucleare, Sezione di Pisa, I-56127 Pisa, Italy
[4] Laboratoire AIM, CEA-IRFU/CNRS/Université Paris Diderot, Service d'Astrophysique, CEA Saclay, 91191 Gif sur Yvette, France
[5] Istituto Nazionale di Fisica Nucleare, Sezione di Trieste, I-34127 Trieste, Italy
[6] Dipartimento di Fisica, Università di Trieste, I-34127 Trieste, Italy
[7] Department of Physics and Astronomy, Rice University, MS-108, P.O. Box 1892, Houston, TX 77251, USA
[8] Istituto Nazionale di Fisica Nucleare, Sezione di Padova, I-35131 Padova, Italy
[9] Dipartimento di Fisica "G. Galilei," Università di Padova, I-35131 Padova, Italy
[10] Center for Space Plasma and Aeronomic Research (CSPAR), University of Alabama in Huntsville, Huntsville, AL 35899, USA
[11] Institut für Astro- und Teilchenphysik and Institut für Theoretische Physik, Leopold-Franzens-Universität Innsbruck, A-6020 Innsbruck, Austria
[12] Istituto Nazionale di Fisica Nucleare, Sezione di Perugia, I-06123 Perugia, Italy
[13] Dipartimento di Fisica, Università degli Studi di Perugia, I-06123 Perugia, Italy
[14] NASA Goddard Space Flight Center, Greenbelt, MD 20771, USA; eleonora.troja@nasa.gov, Julie.E.McEnery@nasa.gov
[15] Department of Physics and Department of Astronomy, University of Maryland, College Park, MD 20742, USA
[16] Santa Cruz Institute for Particle Physics, Department of Physics and Department of Astronomy and Astrophysics, University of California at Santa Cruz, Santa Cruz, CA 95064, USA
[17] Dipartimento di Fisica "M. Merlin" dell'Università e del Politecnico di Bari, I-70126 Bari, Italy
[18] Istituto Nazionale di Fisica Nucleare, Sezione di Bari, 70126 Bari, Italy
[19] Laboratoire Leprince-Ringuet, École polytechnique, CNRS/IN2P3, Palaiseau, France
[20] Institut de Ciencies de l'Espai (IEEC-CSIC), Campus UAB, 08193 Barcelona, Spain
[21] INAF-Istituto di Astrofisica Spaziale e Fisica Cosmica, I-20133 Milano, Italy
[22] Artep Inc., 2922 Excelsior Springs Court, Ellicott City, MD 21042, USA
[23] Department of Physics, Stockholm University, AlbaNova, SE-106 91 Stockholm, Sweden
[24] The Oskar Klein Centre for Cosmoparticle Physics, AlbaNova, SE-106 91 Stockholm, Sweden
[25] Agenzia Spaziale Italiana (ASI) Science Data Center, I-00044 Frascati (Roma), Italy; sarac@slac.stanford.edu
[26] Dipartimento di Fisica, Università di Udine and Istituto Nazionale di Fisica Nucleare, Sezione di Trieste, Gruppo Collegato di Udine, I-33100 Udine, Italy
[27] Space Science Division, Naval Research Laboratory, Washington, DC 20375, USA
[28] Department of Physical Sciences, Hiroshima University, Higashi-Hiroshima, Hiroshima 739-8526, Japan
[29] INAF Istituto di Radioastronomia, 40129 Bologna, Italy
[30] Centre for Astrophysics Research, Science and Technology Research Institute, University of Hertfordshire, Hatfield AL10 9AB, UK
[31] Department of Physics, Center for Cosmology and Astro-Particle Physics, The Ohio State University, Columbus, OH 43210, USA
[32] Science Institute, University of Iceland, IS-107 Reykjavik, Iceland
[33] Research Institute for Science and Engineering, Waseda University, 3-4-1, Okubo, Shinjuku, Tokyo 169-8555, Japan
[34] CNRS, IRAP, F-31028 Toulouse cedex 4, France
[35] Université de Toulouse, UPS-OMP, IRAP, Toulouse, France
[36] Université Bordeaux 1, CNRS/IN2p3, Centre d'Études Nucléaires de Bordeaux Gradignan, 33175 Gradignan, France
[37] Department of Astronomy and Astrophysics, Pennsylvania State University, University Park, PA 16802, USA
[38] Center for Research and Exploration in Space Science and Technology (CRESST) and NASA Goddard Space Flight Center, Greenbelt, MD 20771, USA
[39] Istituto Nazionale di Fisica Nucleare, Sezione di Roma "Tor Vergata," I-00133 Roma, Italy
[40] Department of Physics and Astronomy, University of Denver, Denver, CO 80208, USA
[41] Laboratoire Univers et Particules de Montpellier, Université Montpellier 2, CNRS/IN2P3, Montpellier, France; vlasios.vasileiou@univ-montp2.fr
[42] Hiroshima Astrophysical Science Center, Hiroshima University, Higashi-Hiroshima, Hiroshima 739-8526, Japan
[43] Institute of Space and Astronautical Science, JAXA, 3-1-1 Yoshinodai, Chuo-ku, Sagamihara, Kanagawa 252-5210, Japan
[44] Max-Planck Institut für extraterrestrische Physik, 85748 Garching, Germany

[45] Kavli Institute for Cosmological Physics, University of Chicago, Chicago, IL 60637, USA
[46] Department of Physics, University of Washington, Seattle, WA 98195-1560, USA
[47] NYCB Real-Time Computing Inc., Lattingtown, NY 11560-1025, USA
[48] Department of Physics, Adıyaman University, 02040 Adıyaman, Turkey
[49] Universities Space Research Association (USRA), Columbia, MD 21044, USA
[50] Institució Catalana de Recerca i Estudis Avançats (ICREA), Barcelona, Spain
[51] Consorzio Interuniversitario per la Fisica Spaziale (CIFS), I-10133 Torino, Italy
[52] Dipartimento di Fisica, Università di Roma "Tor Vergata," I-00133 Roma, Italy
[53] Department of Physics and Mathematics, Aoyama Gakuin University, Sagamihara, Kanagawa, 252-5258, Japan
[54] INAF-Istituto di Astrofisica Spaziale e Fisica Cosmica, I-00133 Roma, Italy; luigi.piro@iasf-roma.inaf.it
Received 2011 February 9; accepted 2011 April 28; published 2011 May 26

ABSTRACT

We present the simultaneous *Swift* and *Fermi* observations of the bright GRB 100728A and its afterglow. The early X-ray emission is dominated by a vigorous flaring activity continuing until 1 ks after the burst. In the same time interval, high-energy emission is significantly detected by the *Fermi*/Large Area Telescope. Marginal evidence of GeV emission is observed up to later times. We discuss the broadband properties of this burst within both the internal and external shock scenarios, with a particular emphasis on the relation between X-ray flares, the GeV emission, and a continued long-duration central engine activity as their power source.

Key words: gamma-ray burst: individual (GRB100728A) – radiation mechanisms: non-thermal

Online-only material: color figures

1. INTRODUCTION

The *Fermi Gamma-Ray Space Telescope*, launched in 2008 June, has taken the study of gamma-ray bursts (GRBs) into an energy realm that so far has been poorly explored. *Fermi*/LAT (Large Area Telescope; Atwood et al. 2009) observations of GRBs allow for the first time a detailed study of the temporal and spectral behavior at high energies (>100 MeV). One of the most interesting features is the detection of a delayed and rapidly decaying high-energy (HE) emission, lasting hundreds to thousands of seconds longer than the observed sub-MeV γ-ray emission (Abdo et al. 2009a, 2009b, 2009c). Extended GeV emission, first hinted at in EGRET observations (Hurley et al. 1994), appears now as a common feature of *Fermi*/LAT bursts. The nature of such long-lived HE emission is far from being established. One possibility is that it is generated via synchrotron radiation of the external forward shock (Kumar & Barniol Duran 2009, 2010; Ghisellini et al. 2010). An alternative scenario is that it reflects the gradual turnoff of the central engine activity (Zhang et al. 2011). Such interpretations predict very different afterglow behaviors (Piron & Nakar 2010; Mimica et al. 2010) and therefore can be directly verified through broadband (from optical/X-ray to GeV energies) early-time observations. To date, only one burst (GRB 090510; De Pasquale et al. 2010) of the 20 LAT detected GRBs has been simultaneously detected by the *Swift* multi-wavelength observatory (Gehrels et al. 2004). In this case, an afterglow emission provides a likely explanation of the broadband data set (e.g., De Pasquale et al. 2010; Corsi et al. 2010).

In this Letter, we report on the *Fermi*/LAT detection of a temporally extended emission from GRB 100728A and the simultaneous *Swift* observations of an intense X-ray flaring activity. We further discuss the possibility that in the case of GRB 100728A the observed HE emission is related to X-ray flares and ultimately to the long-lasting activity of the inner engine. Observations and analysis are reported in Section 2; our results are discussed in Section 3; we draw our conclusions in Section 4. Unless otherwise stated, the quoted errors are at the 90% confidence level and times refer to the *Fermi*/Gamma-ray Burst Monitor (GBM) trigger T_0.

2. OBSERVATIONS AND DATA ANALYSIS

2.1. Swift Data

The bright GRB 100728A came into the *Swift* field of view during a slew to a pre-planned target, when the trigger system is disabled. After the spacecraft settled, the burst triggered the Burst Alert Telescope (BAT; Barthelmy et al. 2005) on board *Swift* at 02:18:24 UT on 2010 July 28. *Swift* slewed immediately to the burst. The two narrow field instruments, the X-ray Telescope (XRT; Burrows et al. 2005) and the Ultraviolet Optical Telescope (UVOT; Roming et al. 2005), began settled observations of the field ~80 s after the BAT trigger. An X-ray afterglow was promptly localized at a position of R.A. = $05^h55^m2\overset{s}{.}01$, decl. = $-15°15'19\overset{''}{.}1$ (J2000) with an uncertainty of $1\overset{''}{.}4$ (Beardmore et al. 2010), while no counterpart was observed in the early UVOT unfiltered exposures down to a limiting magnitude $wh > 20.5$ (3σ confidence level; Oates & Cannizzo 2010).

Swift data were analyzed in a standard fashion; we refer the reader to Evans et al. (2007, 2010) for further details. As shown in Figure 1, the early X-ray afterglow (top panel) is characterized by a series of bright X-ray flares superimposed on a power-law decay ($\propto t^{-1.5}$). Each flare can be described by a Fast-Rise Exponential Decay (FRED) profile (solid line) with $0.04 < \Delta t/t < 0.2$. In the same time interval, the BAT light curve (bottom panel) shows a long-lasting emission extending up to ~800 s, with several peaks visible in coincidence with the X-ray flares (vertical dot-dashed lines).

The post-flare X-ray afterglow decays as a power law with slope $\alpha_2 = 1.07 \pm 0.05$, which steepens to $\alpha_3 = 1.63 \pm 0.07$ at $t \sim 10$ ks. No significant spectral evolution is observed. The time-averaged photon index is $\Gamma = -2.07 \pm 0.09$.

By combining the simultaneous BAT and XRT observations, we performed a joint spectral analysis of the X-ray flares. We modeled the absorption with two different components: the

[55] Resident at Naval Research Laboratory, Washington, DC 20375, USA.
[56] Royal Swedish Academy of Sciences Research Fellow, funded by a grant from the K. A. Wallenberg Foundation.
[57] NASA Postdoctoral Program Fellow, USA.

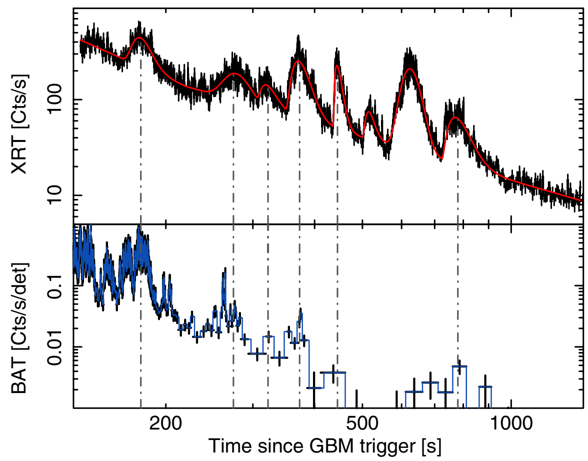

Figure 1. Top panel: early XRT light curve of GRB 100728A. Bottom panel: BAT mask-weighted light curve during the X-ray flaring activity. Several peaks are visible in correspondence of the X-ray flares (vertical dot-dashed lines).

(A color version of this figure is available in the online journal.)

former was fixed at the Galactic value of $N_{\rm H} = 10^{21}$ cm^{-2} (Kalberla et al. 2005) and the latter, representing the absorption local to the burst, was fixed to the value of $N_{\rm H} = 2.6 \times 10^{21}$ cm^{-2} derived from the late-time (10^4–10^6 s) afterglow spectrum. This constraint prevents artificial $N_{\rm H}$ variations caused by the intrinsic spectral evolution, commonly observed in the brightest X-ray flares (Butler & Kocevski 2007). A strong spectral evolution is observed during the first 100 s, showing a peak energy that softens from 95 ± 15 keV during the first flare (from T_0 + 167 s to T_0 + 192 s) to less than 10 keV in the following flares. Excluding the first harder episode, the time-averaged spectrum, from T_0 + 254 s to T_0 + 854 s, is well described by a Band function (Band et al. 1993; $\chi^2 = 614$ for 477 degrees of freedom, dof) with $\alpha = -1.06 \pm 0.11$, $\beta = -2.24 \pm 0.02$, and a peak energy $E_{\rm pk} = 1.0^{+0.8}_{-0.4}$ keV.

2.2. *Fermi* Data

The *Fermi*/GBM triggered and located GRB 100728A at 02:17:31 UT, 53.6 s before the *Swift*/BAT trigger (see Section 2.1). The GBM light curve shows a complex, multipeaked structure with a duration $T_{90} \sim 163$ s in the 50–300 keV energy range (Kienlin 2010). A set of strong peaks is visible at T_0 + 170 s, corresponding to the first flares detected by the XRT. No significant emission above the highly variable background level is detected on longer timescales.

The time-averaged spectrum during the T_{90} interval, from T_0 + 15 s to T_0 + 178 s, can be described with a Band function with the following parameters: $\alpha = -0.58 \pm 0.03$, $\beta = -2.73^{+0.27}_{-0.18}$, and $E_{\rm pk} = 264 \pm 11$ keV (Castor C-statistics 865 for 351 dof). A power-law function with an exponential HE cutoff also provides an adequate description (C-statistics 885 for 352 dof). The event fluence (10–1000 keV) in the selected time interval is $1.181 \pm 0.010 \times 10^{-4}$ erg cm^{-2}. The high fluence of this burst generated an Autonomous Repoint Request, which caused the *Fermi* satellite to slew to the GRB position.

2.2.1. LAT Observations

An unbinned likelihood analysis (Abdo et al. 2009d) was used to search the LAT data for emission from GRB 100728A. As this study is part of a systematic search for HE emission from X-ray flares, a trials factor of 28 for the number of flares considered has to be taken into account in evaluating the detection significances.

Depending on the time window of interest the search was performed on transient-class data, optimally suited for short-duration (tens of seconds) signal-limited studies, or diffuse-class data, best suited for detecting faint emission over longer timescales (Atwood et al. 2009). The analysis included LAT events reconstructed within 15° around the XRT localization (Section 2.1) with energies in the 100 MeV–50 GeV range. The GRB spectrum was modeled using a power law. No point source in the vicinity of the GRB (within 15°) was bright enough to merit inclusion in the background model. The cosmic-ray background and the extragalactic gamma-ray background were estimated following the method described in Abdo et al. (2009d) for the transient-class searches and modeled as a single isotropic power law for the diffuse-class searches. The Galactic diffuse gamma-ray background was described by using the publicly available template produced by the LAT collaboration.[58] The background contribution from the Earth's albedo was negligible since the GRB position was far from the Earth's limb during all the time intervals analyzed. Tests performed with different background models do not show any significant change in our results.

The results of our analysis are summarized in Table 1. A time-resolved search performed on each individual flare did not find any significant excess in the LAT data, though a marginal evidence of emission (test statistic TS > 10, single trial) is present during two of the flares (3 and 6). A time-integrated search performed over the whole flaring interval led to a significant detection (TS = 32 for transient-class events, TS = 42 for diffuse-class events). In this time interval the total number of transient (diffuse) class events is 191 (29); according to the likelihood analysis the number of events associated with the GRB is ∼10 (6). The highest energy diffuse-class event detected during the flaring interval (at T_0 + 709 s) and in spatial coincidence with the source has an energy of 1.68 GeV. The probability of the LAT background producing an event with at least that energy and during the same interval is $\approx 7 \times 10^{-4}$. Events of higher energies, tens of GeV, are detected in the transient-class data set, but the high background rate does not allow us to significantly associate them with the GRB. Our best localization of the LAT emission, derived from transient-class data analysis, is: R.A. = $05^{\rm h}55^{\rm m}49^{\rm s}$, decl. = 15°03′18″, with a statistical uncertainty of 0°.1 (68% confidence level) and a systematic error of 0°.2. This position is consistent with the *Swift* localization (Section 2.1).

In order to determine whether the LAT emission is temporally extended or mainly originated during the higher-significance flares (3 and 6), we performed two stacked searches on the transient-class data set: one aggregating the data during these two flares and one during the whole flaring period excluding the two flares. Emission at a comparable level and with consistent spectral properties is present during both time intervals (see Table 1), therefore we conclude that the LAT emission extends over the whole flaring period. A cross-correlation analysis between the LAT (diffuse-class) and XRT light curves does not detect any significant temporal correlation or anti-correlation between the two data sets. Similar results are obtained from the analysis of the transient-class events.

As shown in Table 1, no emission is detected during the GRB prompt phase. The resulting upper limit is consistent with the extrapolation of the Band spectrum to the LAT energy range. Marginal evidence of emission (TS ≈ 10 for diffuse-class

[58] http://fermi.gsfc.nasa.gov/ssc/data/access/lat/BackgroundModels.html

Table 1
LAT-analysis Results

Temporal Selection	Time Interval (s)	Test Statistic	Flux[a] (10^{-6} ph cm^{-2} s^{-1})	Γ_{LAT}[b]
Flare 1	167–192	0	<28	···
Flare 2	254–304	0	<12	
Flare 3	309–354	11	<30	···
Flare 4	359–414	0	<12	···
Flare 5	439–474	0	<15	···
Flare 6	504–544	11	<30	···
Flare 7	577–694	0	<7	···
Flare 8	724–854	0	<4	···
Time-integrated Search				
Pre-flares (prompt)	0–167	5	<18	···
Post-flares[c]	854–1654	10	0.7 ± 0.5	-1.4 ± 0.4
X-ray flares	167–854	32	2.4 ± 1	-1.4 ± 0.2
X-ray flares	254–854	27	2.0 ± 1	-1.3 ± 0.3
Flares 3 and 6	···	22	9.6 ± 5	-1.2 ± 0.3
Flaring Interval (excluding 3 and 6)	···	17	1.6 ± 1	-1.6 ± 0.4

Notes.
[a] Fluxes in the 100 MeV–50 GeV energy band. The quoted errors are at the 68% confidence level. Upper limits are at the 95% confidence level and were calculated using the best-fit photon index $\Gamma_{LAT} = -1.4$.
[b] Here the photon index Γ_{LAT} is defined such that $dN/dAdEdt \propto E^{\Gamma_{LAT}}$.
[c] From diffuse-class LAT data.

events) is present after the end of the observed X-ray flaring activity.

3. DISCUSSION

Below we summarize the results that are relevant to address the origin of the GeV emission.

1. Significant GeV emission is found in the same interval where the X-ray flaring activity is enhanced. However, the backgrounds and limited statistics in the LAT data do not allow us to search for a one-to-one correlation between the GeV emission and the single flare episodes. There is marginal evidence of GeV emission after the end of the flaring period.
2. The GeV flux is consistent with the extrapolation of the power law describing the flare spectrum above 1 keV. Assuming that an afterglow component is present below the flares and that it has the same spectrum observed at later times, it is found that the GeV flux is also consistent with the extrapolation of this putative component. The LAT data exhibit a harder spectrum than that observed in X-rays (see Figure 2), though marginally consistent (within 3σ) with the X-ray spectral slope.

The last result suggests that the HE emission can simply represent the HE tail of the synchrotron component. The presence of an additional Inverse Compton (IC) component dominating over the synchrotron just above ~1 GeV cannot be excluded, and it would be consistent with the observed flatter GeV spectrum. These deductions apply to whichever is the source of electron acceleration, internal or external shocks.

The discovery of HE emission in a time frame of vigorous flaring activity in X-rays lead us to consider first the association of the GeV emission with X-ray flares. We now discuss this scenario. Given the large number of flares, we can exclude that a delayed external shock is the dominant process originating the X-ray flares (Galli & Piro 2007). In fact, in this model only a single outstanding flare, corresponding to the onset of the afterglow from a long-duration central engine, is produced.

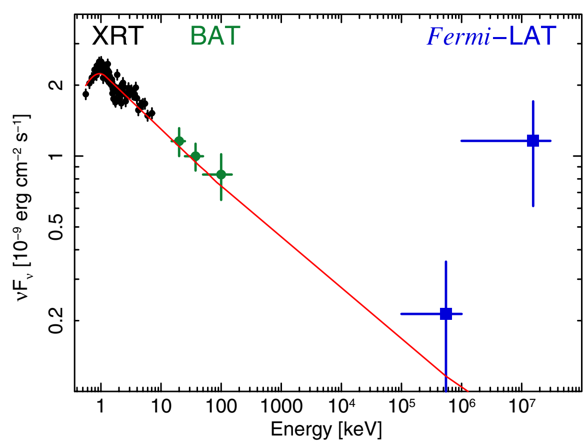

Figure 2. Spectral energy distribution of the X-ray flares including data from *Swift*/BAT, XRT, and *Fermi*/LAT. Error bars are at 1σ confidence level. The solid line shows the best-fit model of the joint XRT/BAT spectral fit described in Section 2.1 and extrapolated to the *Fermi*/LAT energy range. As discussed in the text, the *Fermi*/LAT detection is consistent within 3σ with the extrapolation of the model.

(A color version of this figure is available in the online journal.)

We thus consider internal shocks from a long-lasting relativistic outflow as the source of flares (e.g., Zhang et al. 2006).

In order to allow the GeV emission to be observed we require two conditions. First, the source has to be optically thin for pair production. By computing the optical depth for e^+e^- production (Lithwick & Sari 2001) by photons of energy E_{GeV} in GeV on the X-ray to GeV power-law component observed at about 300 s, we derive a lower limit on the Lorentz factor:

$$\Gamma \geqslant \Gamma_{\gamma\gamma} \approx 30\, E_{GeV}^{1/6}\, t_v^{-1/6} D_{28}^{1/3} \left(\frac{1+z}{2}\right)^{1/3}, \quad (1)$$

where we specialized the equation for a photon index 2. The tightest constraints on Γ are derived from the shortest timescale for variability t_v that can be associated with the relativistic flow produced by the central source. In the scenario of a late internal shock, X-ray flares and the GRB prompt emission are both related to the central engine activity. We therefore consider that a variability timescale of millisecond typical of the prompt phase is a reasonable possibility. In this case, a single flare is produced by the superposition of several internal shock events from a relativistic wind active for the whole duration of the flare. By assuming $t_v = 10^{-3}$ s, a timescale similar to that characterizing the prompt phase, one derives $\Gamma_{\gamma\gamma} \sim 115\, E_{\rm GeV}^{1/6}$ for a typical redshift $z = 1$. On the contrary, if the flare is associated with a single internal shock event, i.e., the interaction of two shells, then t_v should be equal to the flare duration, i.e., about 100 s. In this case $\Gamma_{\gamma\gamma} \sim 20\, E_{\rm GeV}^{1/6}$.

The lower boundary on the Lorentz factor derived above for the flaring phase encompasses the range of values typical of the prompt phase (Lithwick & Sari 2001; Liang et al. 2010), consistent with the notion that a long-duration relativistic outflow with a Lorentz factor of the order of ≈100 is producing both the prompt emission and the flares. In principle, the parameters describing the relativistic shocks ($\epsilon_e, \epsilon_B, L, \Gamma, t_v$) can all be time dependent, i.e., be different during the prompt and late flaring phases. On the other hand, one wishes to reduce the number of variable parameters (Occam's razor). It goes beyond the scope of this Letter to find the best self-consistent internal shock model reproducing both the prompt and X-ray flaring phases. We just note the following. The model should be able to reproduce a peak energy that shifts from the ≈100 keV region during the prompt phase to the keV range observed during X-ray flares. Recalling that the peak of the synchrotron spectrum is given by (e.g., Zhang & Mészáros 2002)

$$\nu_m \propto \epsilon_e^{3/2}\epsilon_B^{1/2}L^{1/2}\Gamma^{-2}t_v^{-1}, \tag{2}$$

it follows that the decrease of the luminosity L from the prompt to the flare phase already accounts for a decrease of the peak energy by a factor of 20, with all the other parameters remaining constant. The further reduction that is needed can be obtained, e.g., by the very reasonable assumption that the magnetic field weakens at the larger radii where flares are produced or by a smaller contrast in the Lorentz factor between colliding shells (Barraud et al. 2005).

The second condition is derived by requiring that the maximum energy at which the electrons are accelerated is large enough to produce photons of energy E via synchrotron radiation:

$$\Gamma > 60\left(\frac{1+z}{2}\right)(1+Y)E_{\rm GeV}, \tag{3}$$

where Y is the Compton y parameter. This equation gives a condition on Γ comparable to that derived from Equation (1). In conclusion, we find that both the prompt emission and the later X-ray flares and HE emission can be explained by internal shocks produced by a long-duration central engine with a Lorentz factor of ≈ 100 and decreasing luminosity.

This simple internal shock model predicts an emission that is cospatial and simultaneous in the X-ray and GeV ranges. On the other hand, we find a marginal evidence of delayed HE emission. This is naturally predicted when the X-ray photons, produced by internal shocks at smaller radii, are upscattered to GeV energies via IC by the electron population of the forward shock (Wang et al. 2006; Fan et al. 2008).

Finally, given the quality of the present data set, we cannot exclude the possibility that the GeV emission is actually related to an afterglow underlying the X-ray flares. This requires that the afterglow onset takes place before 200 s. Such a condition is satisfied when the Lorentz factor of the relativistic flow at the beginning of the deceleration phase is

$$\Gamma_{\rm ext} > \begin{cases} 171\left(\frac{1+z}{2}\right)^{3/8}\left(\frac{E_{54}}{n}\right)^{1/8} & \text{ISM,} \\ 74\left(\frac{1+z}{2}\right)^{1/4}\left(\frac{E_{54}}{A^*}\right)^{1/4} & \text{Wind,} \end{cases} \tag{4}$$

where A^* is the density scaling factor in units of 5×10^{11} g cm^{-1}. In other GRBs, the HE emission has been indeed associated with the forward shock synchrotron emission (Ghirlanda et al. 2010; Kumar & Barniol Duran 2010), though the shorter timescales observed require much larger values of $\Gamma_{\rm ext}$ than those derived here. We further explore the external shock scenario in GRB 100728A by analyzing the late-time X-ray behavior. The afterglow spectral and temporal laws are bound to obey specific relations (the so-called closure relations, e.g., Zhang & Mészáros 2004) that depend upon the density profile of the external medium, the jet opening angle, and the relative position of the typical frequencies of the synchrotron spectrum with respect to the observed range. Within the simple external shock model, the closest solution envisages a jet with a rather narrow opening angle of ≈1–2 deg expanding in a medium with a wind-like density profile, though the lack of multi-wavelength afterglow observations does not allow us to firmly characterize the circumburst environment. This scenario is consistent with the lack of spectral variations before and after the break at 10 ks, albeit in a wind-like medium a jet transition is expected to take place on much longer timescales (Kumar & Panaitescu 2000). In this scenario the cooling frequency falls below the X-ray band, and the early GeV emission (if afterglow) likely belongs to the same synchrotron regime. In this case, the LAT emission should display a similar decay slope of ∼1.07 and a photon index of ∼−2.07, softer than the observed value of -1.4 ± 0.2 (1σ) but still consistent within the large uncertainty.

4. CONCLUSION

GRB 100728A is the second case to date with simultaneous *Swift* and *Fermi* observations. HE gamma rays are detected by the *Fermi*/LAT until 850 s (TS = 42) and possibly continuing until 1600 s (TS ≈ 10). Very interestingly, the early X-ray afterglow exhibits intense and long-lasting flaring activity, visible both in BAT and XRT. Although an afterglow origin of the GeV emission cannot be excluded, the presence of bright X-ray flares unveiled by *Swift* observations opens the possibility that a prolonged central engine activity is powering the temporally extended HE emission observed in this burst.

Within the internal shock scenario a relativistic outflow with a Lorentz factor of ≈ 100 and decreasing luminosity can explain the prompt emission, the later X-ray flares, and HE emission. The presence of a delayed HE emission naturally arises from IC scattering of low-energy flare photons off the relativistic electrons at the external forward shock radius.

We thank the referee for a careful reading of the Letter and a rapid reply.

E.T. was supported by an appointment to the NASA Postdoctoral Program at the Goddard Space Flight Center, administered by Oak Ridge Associated Universities through a contract with NASA.

The *Fermi* LAT Collaboration acknowledges support from a number of agencies and institutes for both the development and the operation of the LAT as well as scientific data analysis.

These include NASA and DOE in the United States, CEA/Irfu and IN2P3/CNRS in France, ASI and INFN in Italy, MEXT, KEK, and JAXA in Japan, and the K. A. Wallenberg Foundation, the Swedish Research Council, and the National Space Board in Sweden. Additional support from INAF in Italy and CNES in France for science analysis during the operations phase is also gratefully acknowledged.

REFERENCES

Abdo, A. A., et al. 2009a, ApJ, 706, L138
Abdo, A. A., et al. 2009b, Nature, 462, 331
Abdo, A. A., et al. 2009c, Science, 323, 1688
Abdo, A. A., et al. 2009d, ApJ, 707, 580
Atwood, W. B., et al. 2009, ApJ, 697, 1071
Band, D., et al. 1993, ApJ, 413, 281
Barraud, C., Daigne, F., Mochkovitch, R., & Atteia, J. L. 2005, A&A, 440, 809
Barthelmy, S. D., et al. 2005, Space Sci. Rev., 120, 143
Beardmore, A. P., Evans, P. A., Goad, M. R., & Osborne, J. P. 2010, GCN Circ., 11005
Burrows, D. N., et al. 2005, Space Sci. Rev., 120, 165
Butler, N. R., & Kocevski, D. 2007, ApJ, 663, 407
Corsi, A., Guetta, D., & Piro, L. 2010, ApJ, 720, 1008
De Pasquale, M., et al. 2010, ApJ, 709, L146
Evans, P. A., et al. 2007, A&A, 469, 379
Evans, P. A., et al. 2010, A&A, 519, A102
Fan, Y., Piran, T., Narayan, R., & Wei, D. 2008, MNRAS, 384, 1483
Galli, A., & Piro, L. 2007, A&A, 475, 421
Gehrels, N., et al. 2004, ApJ, 611, 1005
Ghirlanda, G., Ghisellini, G., & Nava, L. 2010, A&A, 510, L7
Ghisellini, G., Ghirlanda, G., Nava, L., & Celotti, A. 2010, MNRAS, 403, 926
Hurley, K., et al. 1994, Nature, 372, 652
Kalberla, P. M. W., et al. 2005, A&A, 440, 775
Kienlin, A. v. 2010, GRB Coordinate Network, 11006, 1
Kumar, P., & Barniol Duran, R. 2009, MNRAS, 400, L75
Kumar, P., & Barniol Duran, R. 2010, MNRAS, 409, 1243
Kumar, P., & Panaitescu, A. 2000, ApJ, 541, L9
Liang, E., et al. 2010, ApJ, 725, 2209
Lithwick, Y., & Sari, R. 2001, ApJ, 555, 540
Mimica, P., Giannios, D., & Aloy, M. A. 2010, MNRAS, 407, 2501
Oates, S. R., & Cannizzo, J. K. 2010, GCN Circ., 11016
Piran, T., & Nakar, E. 2010, ApJ, 718, L63
Roming, P. W. A., et al. 2005, Space Sci. Rev., 120, 95
Wang, X., Li, Z., & Mészáros, P. 2006, ApJ, 641, L89
Zhang, B., & Mészáros, P. 2002, ApJ, 581, 1236
Zhang, B., & Mészáros, P. 2004, Int. J. Mod. Phys. A, 19, 2385
Zhang, B., et al. 2006, ApJ, 642, 354
Zhang, B., et al. 2011, ApJ, 730, 141